ELSEVIER

Atmospheric Research 38 (1995) 333–350

ATMOSPHERIC RESEARCH

Microphysical characteristics of monsoon clouds and cloud sublayers as revealed by the MONEX aircraft observations

G.V. Rao *, R.D. Tamin [1]

Department of Earth and Atmospheric Sciences, Saint Louis University, St. Louis, Missouri, USA

Accepted 4 November 1994

Abstract

The summer monsoon atmosphere was subjected to aerial cloud microphysical measurements by the National Center for Atmospheric Research (NCAR)'s Electra as part of the Arabian Sea component of the Summer Monsoon Experiment (SMONEX). The Particle Measuring System (PMS)'s probes were mounted on these flights. This study documents vertical profiles and concentration counts of aerosols and precipitation size particles for the flights on 20 and 24 June 1979. These flights were selected because the meteorology associated with them was analyzed in detail by several investigators who were interested in the turbulence flux measurements which were unique to these flights. The samples on 20 June were collected mostly underneath clouds except once within a cloud. In contrast, they were gathered exclusively within clouds on 24 June. The observations on these two days were collected in four different locations over the Arabian Sea when organized convection was presented.

Results show that the aerosol concentration counts as measured by the ASAS-probe were higher than those expected from measurements in suppressed convective conditions. The ASAS and FSSP readings were nearly constant in the boundary layer. The FSSP readings increased more than ASAS readings with height passing them at elevations greater than 1500 m. Some young clouds with a depth of 1600 m showed maximum updraft values occurring at a certain level (e.g., 1000 m). At this level, a maximum concentration of droplets belonging to a particular size group (≈ 15 μm) was found. Thus a positive association was seen between these droplets and the vertical velocity distribution.

1. Introduction

Although the structure of monsoon disturbances is widely known (see the studies reviewed by Hastenrath, 1991) the distributions of aerosols and fine cloud droplets as

* Corresponding author.

[1] Current affiliation: Agency for the Assessment and Application of Technology, Jakarta, Indonesia.

SSDI 0169-8095(95)00004-6

measured by the ASAS and FSSP probes over the monsoon seas and within monsoon clouds are poorly documented. In June 1979, some cloud physics measurements were made in conjunction with the Summer Monsoon Experiment (SMONEX). For details on SMONEX see Fein and Kuettner (1980). Although these measurements are several years old, they are worthy of further analysis and discussions, because practically no in situ cloud physics observations exist over the Arabian Sea. As is well known, this sea develops strong winds during the monsoon onset. Besides, interest is growing among the scientific community to observe clouds in the tropics in view of El Niño and its impact on world-wide weather, including the Indian monsoon. The efforts of cloud physics and boundary layer investigators complemented each other during two specific flights of Electra of the National Center for Atmospheric Research [2]. These flights occurred on 20 and 24 June 1979 over the eastern and central Arabian Sea. Valuable wind including turbulence measurements, thermodynamic and cloud physics data were gathered. The wind and thermodynamic data collected on these two flights were analyzed and the structure of monsoon flow discussed by several investigators (e.g., Holt and Raman, 1985; Meyer and Rao, 1985 and Rao and Hor, 1991). In the following, the aerosol and small cloud-drop distributions in the vertical on both days and underneath clouds and once within a cloud on 20 June and at three levels within clouds on 24 June were analyzed.

The objectives of this research are: (a) to furnish the vertical distributions and concentration counts of giant aerosols, haze droplets and small cloud droplets, as measured by ASAS (Active Scattering Aerosol Spectrometer) and FSSP (Forward Scattering Spectrometer Probe), in the free atmosphere as well as within the monsoon boundary layer and also within clouds when organized convection was present; (b) to relate the distribution of small cloud dropletsize particles as measured by FSSP to the internal structure of clouds and (c) to discuss the vertical variation of the mean updrafts and down drafts in monsoon clouds and relate such variation, if possible, to the vertical distribution of cloud droplets.

2. Aerial exploration and flight cross sections

Generally, with monsoon onset, disturbed conditions prevail in the central and eastern Arabian Sea. This was true for 1979 as well, when monsoon onset occurred over southern India soon after 11 June; several cloud clusters with embedded bands dominated the EAS (Benson and Rao, 1987) on 20 June. Fig. 1 shows the horizontal projection of the Electra flight path on this day. The research aircraft Electra performed racetrack manœuvers near 11°N and 71°E (Electra South). These manœuvers were oriented along WNW–ESE. The mean wind speed and direction along these flights were 8.6 m s^{-1} and 240°. Subsequently, the aircraft executed stair step runs at alternating altitudes of 100 and 500 m. Finally, it performed a second series of racetrack runs near 15°N and 69°E (Electra North). The mean wind speed and direction along these flights were 16.2 m s^{-1} and 260°.

Fig. 2 shows a cross-sectional projection of the flight track for 20 June. The descent shown in Fig. 2 and also mentioned in Table 1 began at 0526 UTC. Subsequently, the level

[2] Operated by the University Corporation for Atmospheric Research and sponsored by the National Science Foundation.

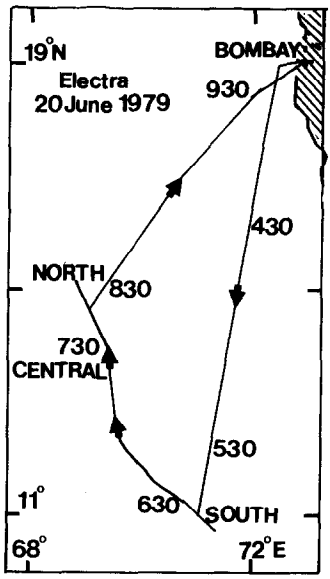

Fig. 1. Flight track of Electra on 20 June 1979. Times indicated are in UTC, which is 5.5 h behind Indian Standard Time. Spatial locations of Electra South, Central and North are shown.

flights, at approximate horizontal distances of 5700 m relating to Electra South, Central and North, were executed. Finally, the aircraft ascended at 0822 UTC and returned to Bombay. All these flights occurred in a generally disturbed synoptic situation. The South and Central runs took place in rain underneath clouds. In the North area, marked development of clouds was seen. The flight there at 475 m occurred in no rain but underneath clouds, the flight at

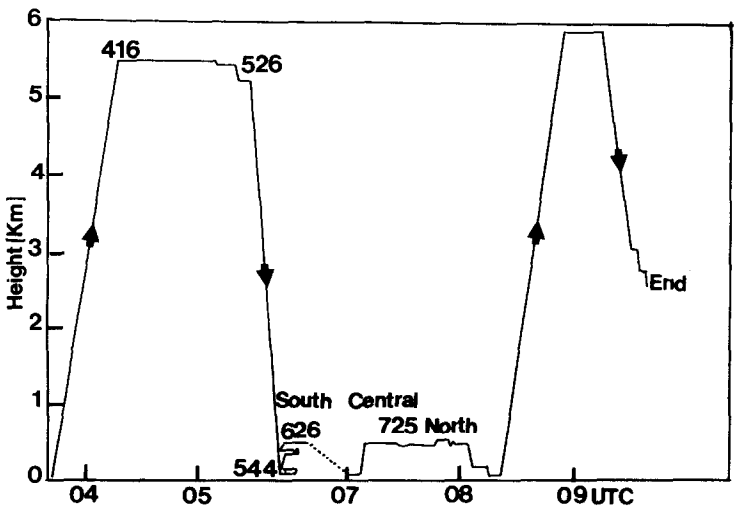

Fig. 2. A cross-sectional projection of Electra flight on 20 June. Time locations of Electra South, Central and North are shown.

Table 1
Starting time (Universal Coordinated Time, UTC), duration and mean elevation of each flight on 20 June 1979 for which aerosol and cloud microphysics measurements were available

Start (UTC)	Duration (min)	Flight level (m)	Electra run	Comment
5:26	18	3170–80	descent	
6:26	6	485	S	In rain, but not in clouds
7:25	8	475	C	In rain, but not in clouds
7:41	5	475	N	In no rain, but underneath clouds
7:47	4	540	N	Within a cloud near its base
7:58	6	500	N	In rain, but not in clouds
8:22	31	90–5900	ascent	

500 m occurred in rain, just under a cloud base. The flight at 540 m was executed within a cloud near its base. Finally, the aircraft ascended to 5900 m and returned to Bombay.

Fig. 3 shows the horizontal projection of the flight path on 24 June. The first series of racetrack maneuvers took place near 17°N and 70°E (Electra East). In this general area, the cloud bands were in existence by 0300 UTC. Some of the tops of the bands exceeded 5 km. These flights were oriented roughly N–S. The mean wind speed and direction were 11.3 m s^{-1} and 250°. The second series of racetrack runs took place near 17°N and 64°E (Electra West). These flights were oriented along NNW–SSE. The mean wind speed was 16.5 m s^{-1} and direction 242°.

Fig. 4 shows a cross-sectional projection of the flight track for 24 June. Highlights are the descent at 0436 UTC, the three Electra East level flights between 0513 and 0529 UTC within clouds, the three Electra West level flights between 0752 and 0810 UTC also with clouds, and the ascent from 0817 to 0850 UTC. Table 2 shows the level flights covered nominal distances of 6 km.

On both 20 and 24 June, the Electra flights were dedicated to an exploration of the monsoon boundary layer. Auxiliary measurements of cloud microphysics were made also. Since convection was not specially targeted for reconnaissance, it was not well sampled possibly in this study. Nevertheless the flights were unique, because aerosol and small cloud droplet size distributions in the vertical in this part of the tropics is not available. Such

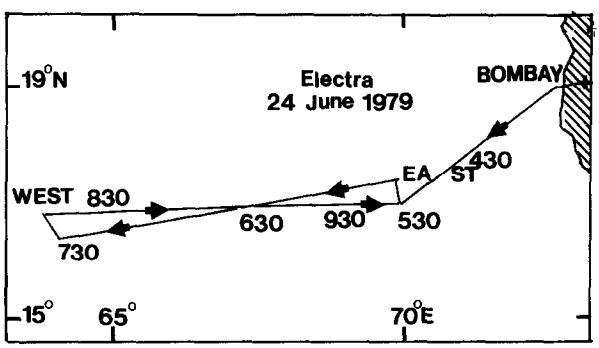

Fig. 3. Flight track of Electra on 24 June. Spatial locations of Electra East and West are shown.

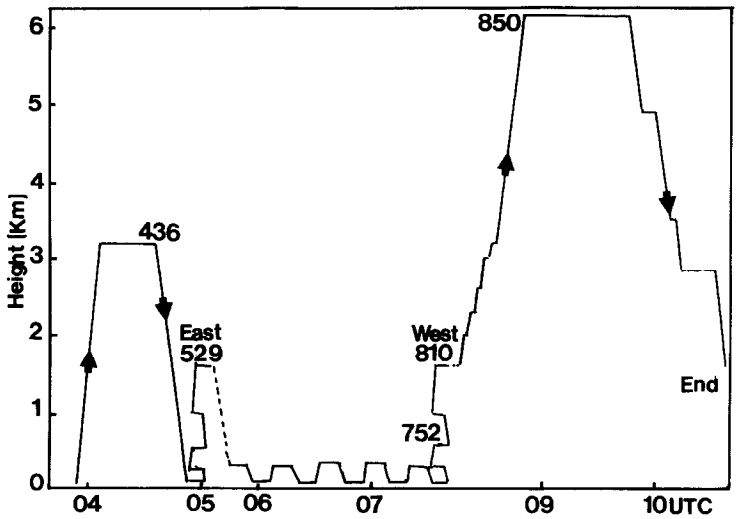

Fig. 4. Same as Fig. 2, except it relates to 24 June. Time locations of Electra East and West are shown.

Table 2
Starting time, duration, and mean elevation of each flight on 24 June 1979 for which aerosol and cloud microphysics measurements were available. Flights marked E and W occurred in clouds

Start (UTC)	Duration (min)	Flight level (m)	Electra run
4:36	17	3170–80	descent
5:13	6	540	E
5:21	6	1000	E
5:29	8	1610	E
7:52	7	590	W
8:01	7	1000	W
8:10	7	1610	W
8:17	33	1610–6150	ascent

distributions are becoming under increasing scrutiny as a result of El Niño and its impact on worldwide weather including the Indian monsoon.

3. Microphysical measurements and data quality

Techniques for measuring hydrometeors have advanced significantly in 1960's and 1970's. The wide range of sizes of interest (10^{-1} to 10^{4} μm) and the number densities preclude any one instrument to record the whole range. A research aircraft because of its mobility is ideal to measure the size spectra. The principle behind the PMS probes had been discussed by Knollenberg (1981). The details of the PMS probes and their installation was discussed by Baumgardner (1989). These probes were located in the forward top portion of the fuselage in 1979. This location was found to be not ideal, because the streamlines of

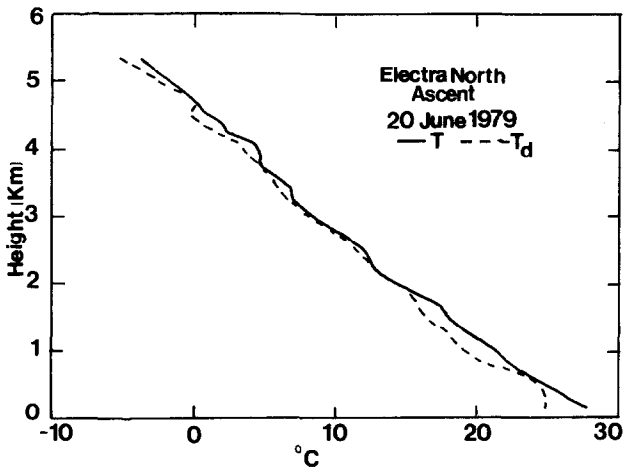

Fig. 5. Temperature and dewpoint temperature profiles based on the ascent at Electra North on 20 June. See Figs. 1 and 2 for the location of Electra North.

particles flowing around and over the nose and cockpit suffered a deflection and converged to a location close to that of the pylon-mounted PMS probes. Therefore, it was likely that an exaggerated concentration of large cloud drops resulted (Spyers-Durran, 1993). In the following, we discussed only one measurement (with X-200 and Y-200) dealing with precipitation sized particles. Most of the discussion hovered around the results of ASAS and FSSP measurements, which apparently did not suffer from the above drawback. With these probes for the level flights the measurements inside and underneath clouds were clearly distinguished. No corrections were made to the PMS data while they were processed at NCAR. Because the concentrations discussed were small, the corrections are likely to be minor. For example, Baumgardner (1989) mentions corrections exceeding 10% were warranted when the concentrations were more than 300 cm^{-3}. In this study, the total concentrations for each of the ASAS and FSSP probes were around 100 cm^{-3}. For these probes, possible errors in the measurements are the undersizing due to the short transit times through the probes; see (Cerni, 1983; Baumgardner, 1987). However, no corrections were made to account for this possible error. In the following, it was ensured that all time periods of study registered continuous measurements. We omitted segments of runs which indicated no

Table 3
Specification of PMS probes listing their size ranges and resolutions (Baumgardner, 1989)

Instrument	Measurement range			Nominal bin width
	μm	μm		
ASAS	0.12–	3.12	diameter	(0.2 μm)
FSSP	2.00–	32.00	diameter	(2.0 μm)
X-200	40.00–	280.00	diameter	(20 μm)
Y-200	300.00–	4,500.00	diameter	(300 μm)

readings or detected very few drops. It was assumed that stable results were acquired in the following by plotting data from various probes and ensuring continuity from one probe to the next one.

The PMS probe data were available either in printed form at one second interval or in plots in the form of histograms for each bin at one minute intervals. The histograms provided our basic data. The time intervals shown in Tables 1 and 2 were chosen after insuring homogeneity of the sample (collected in cloudy areas or in clear areas which was exclusively based on cameras mounted on the aircraft, observers' logs, and radiation measurements). Data from cloudy and clear areas were not mixed. The histogram data were summed over the time interval, for each bin, but averaged with respect to time and shown in Figs. 12–17. On the other hand, the vertical distributions shown in Figs. 6, 9 and 11 were based on the integrated bin totals for each probe at one minute intervals. Height was expressed in terms of time and the profiles of ASAS and FSSP were shown. Temperature T and dew point temperature T_d were also shown in a similar fashion in Figs. 5, 8 and 10.

Table 3 shows that ASAS has a range of 0.12–3.12 μm and FSSP from 2 to 32 μm (although other ranges are possible). The instruments ASAS and FSSP can typically measure the mean, mode, and median volume diameters using bin widths varying from 0.5 to 2 μm, respectively.

Generally, precipitation hydrometeors (measured with Y-200 probe) are sized with lower percentage errors than cloud droplets (measured with X-200 probe). Individual particle tolerances are typically 10% of size.

4. Vertical profiles

To interpret the vertical profiles of ASAS and FSSP properly, it is helpful to have temperature and moisture distributions. Such distributions for Electra North were displayed in Fig. 5, (see Figs. 1 and 2 for the location of Electra North) on 20 June. Several layers of

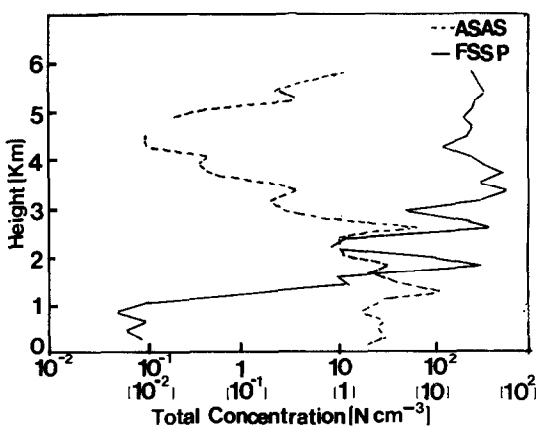

Fig. 6. ASAS and FSSP profiles based on the Electra North ascent referred to in Fig. 5.

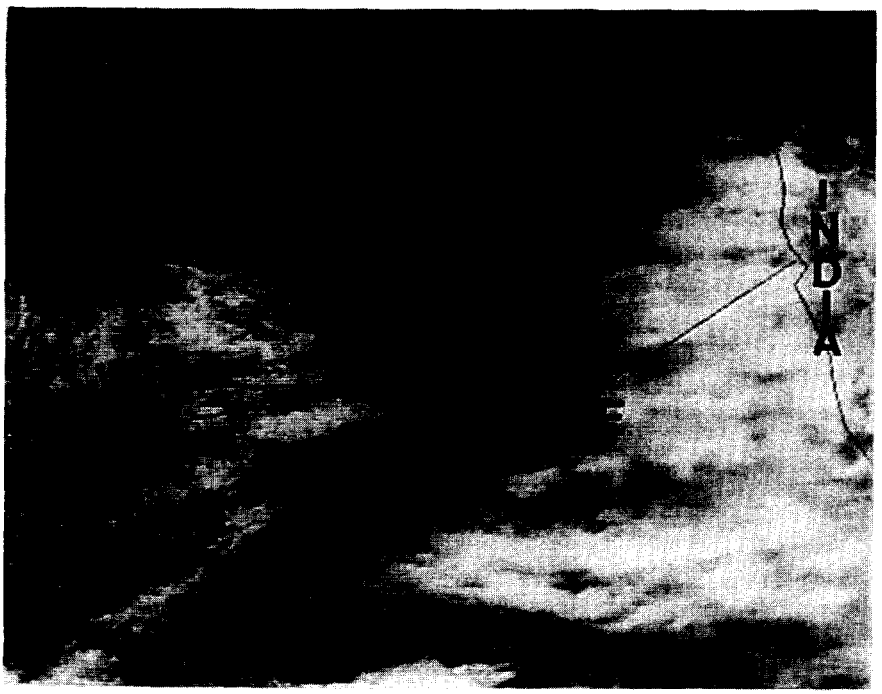

Fig. 7. Satellite Vis imagery for 0700 UTC 24 June showing the cloudiness over Electra East and over Electra West. The bands over East are deep as shown by the Cirrus outflow while those over West are relatively shallow.

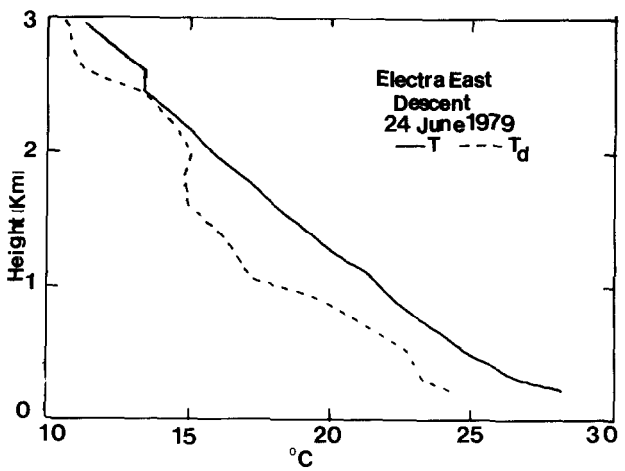

Fig. 8. Temperature and dewpoint temperature profiles based on the descent at Electra East on 24 June. See Figs. 3 and 4 for the location of descent.

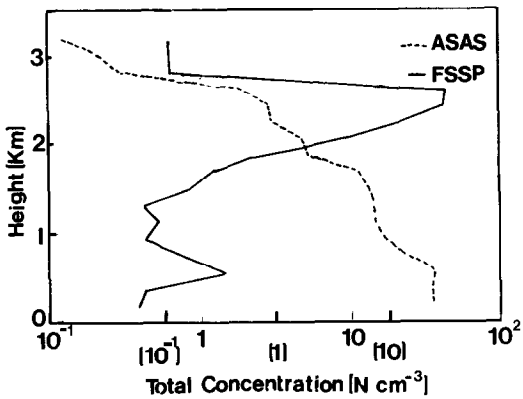

Fig. 9. ASAS and FSSP profiles based on the Electra East descent referred to in Fig. 8. Abscissa for FSSP in parenthesis.

near saturation were shown. Examples are 500 to 875 m, 1875 to 3250 m and higher up. The dry layer from 875 to 1750 m coincided with the region where weak northerlies prevailed. This is understandable because northerlies, coming from the land area, are relatively dry.

The ASAS and FSSP profiles for this Electra North ascent sounding were shown in Fig. 6. Nearly constant values were indicated up to 900 m. This level described the Low-Level Westerly Jet Stream maximum (not shown). Apparently, well mixed conditions existed within the layer of maximum winds. Subsequently, the ASAS showed an increase to 100 cm^{-3} at about 1200 m. A dry layer existed in this vicinity followed by a moist layer. The FSSP profile also showed a nearly constant value in the lower levels and then increased to 50 cm^{-3} to about 1750 m. After about 2500 m, however, the ASAS continued to decline

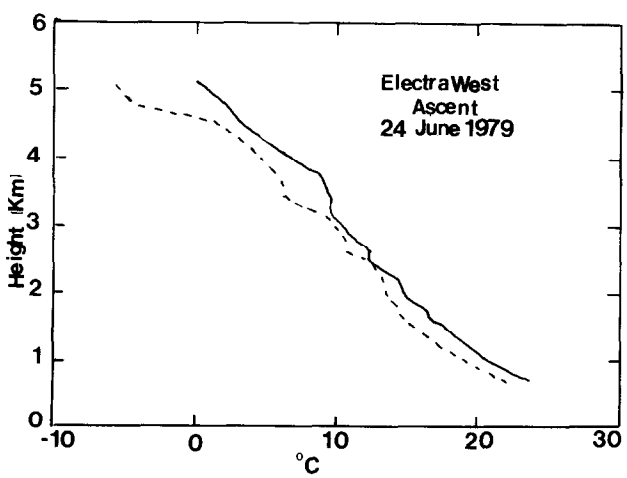

Fig. 10. Temperature and dewpoint temperature profiles based on the ascent at Electra West on 24 June. See Figs. 3 and 4 for the location of ascent.

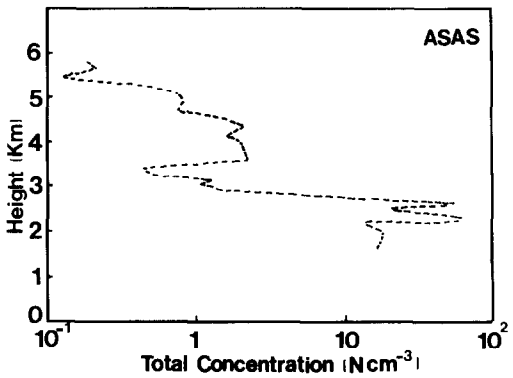

Fig. 11. ASAS and FSSP profiles based on the Electra West ascent referred to in Fig. 10.

while the FSSP remained nearly constant. In general, both ASAS and FSSP showed different layers where maxima were reached. This was seen more clearly above the boundary layer.

Fig. 7 shows a general distribution of clouds on 0700 UTC 24 June 1979 over the Arabian Sea as revealed by the Vis imagery of GOES satellite. Of interest, are the locations of Electra East and West. Flying from Bombay, the aircraft traveled through deep clouds (as disclosed by the return leg at Electra West, tops near 6000 m). The descent sounding of T and T_d (Fig. 8) showed a moist layer from 2500 and 2000 m and then a relatively dry layer from 1750 to 1000 m. Fig. 9 shows the ASAS and FSSP readings in the Electra East area. The ASAS readings were nearly constant in the low levels up to 500 m and then fell, but showed several layers. The FSSP registered a remarkable increase from 1250 to 2500 m. In the general layer (2000–2500 m), the Liquid Water Content (LWC) was high (1.4 gm m^{-3}, not shown) confirming the existence of a cloud there. The LWC's were also high locally at 750 and 1700 m. It appears that FSSP values overtook the ASAS values at about 2000 m.

Fig. 10 shows that ascent soundings of T and T_d in the Electra West area. See Figs. 3 and 4 for the location of Electra West. Near saturation conditions existed from 2250 to 3100 m. Only ASAS readings were available (Fig. 11), which confirm relatively high values coinciding with the beginning and ending of saturation conditions.

5. Results based on level runs

The ordinate of the figures in this section represents the change in concentration ΔN, over a bin width, ΔS. The abscissa shows the mean size. As mentioned in Section 3, these data were available as plots for each minute. We summed them over the respective time interval shown in Tables 1 and 2, but averaged them over one minute interval and presented the results. Fig. 12 shows the five aerosol distributions, as measured by the ASAS probe, at slightly different altitudes but generally in the vicinity of 480 m. To save space, the Electra North ordinate was staggered and is shown in parenthesis. In the general area of Electra South and North, uniform concentrations were shown indicating that the airmass studied

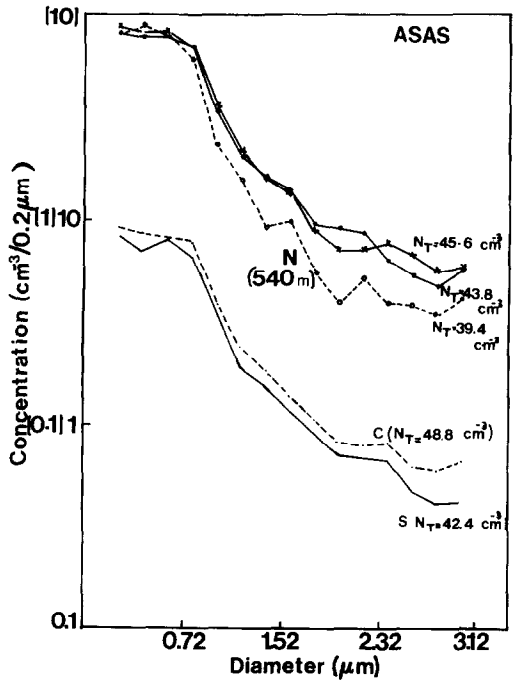

Fig. 12. Size distribution of aerosols using ASAS for Electra South (S), Central (C) and North (N) for 20 June. Ordinate for Electra (N) is shown in parenthesis. For Electra (S), solid represents 485 m; for Electra (C), dashed represents 475 m; and for Electra (N), dots represent 475 m; stars, 500 m, circles, 540 m. Total number concentration, N_T(N cm^{-3}) are shown for each run. See Figs. 1 and 2 for the locations of S, C and N. The S and C runs were executed in rain but not in clouds; the 475 m run of North occurred in no rain and also not in clouds; the 500 m flight of North took place in rain but not in cloud; and finally, the 540 m run of North was executed in a cloud close to its base.

was homogeneous. The spectral distributions also showed a similarity in slope and pointed at an exponential decrease of aerosols larger than 0.8 micron. The total concentration for each run varied from 39 to 48 cm^{-3}. These values may be compared with Podzimek (1973)'s values varying from 0.09 to 15 cm^{-3} on the islands along southern Texas and the values of Pruppacher and Klett (1987), for $r > 0.03$ μm, of 5 cm^{-3} over the Indian Ocean based on ship observations. Ellingson and Serafino (1984) reported about 1.2 cm^{-3} in the spectral range 0.5–1.0 μm and 0.6 cm^{-3} in the range 0.1–1.52 μm in suppressed convection over the Arabian Sea. The difference between these values and ours is understandably due to the differing ranges of integration. The meteorological condition was also a factor. All our observations excepting one (540 m, N) were taken exclusively underneath cloud bases in strong wind regimes (speeds exceeding 8.6 m s^{-1}). The 540 m run was executed within a cloud.

The readings of the next higher probe, FSSP, are shown in Fig. 13. An exponential fall in the concentration was indicated with diameter. In general, the slopes were similar and agreed fairly up to 14 μm as a continuation of the slope from the ASAS results. The Electra South total concentrations averaged 0.2 cm^{-3}, while Electra North registered higher counts

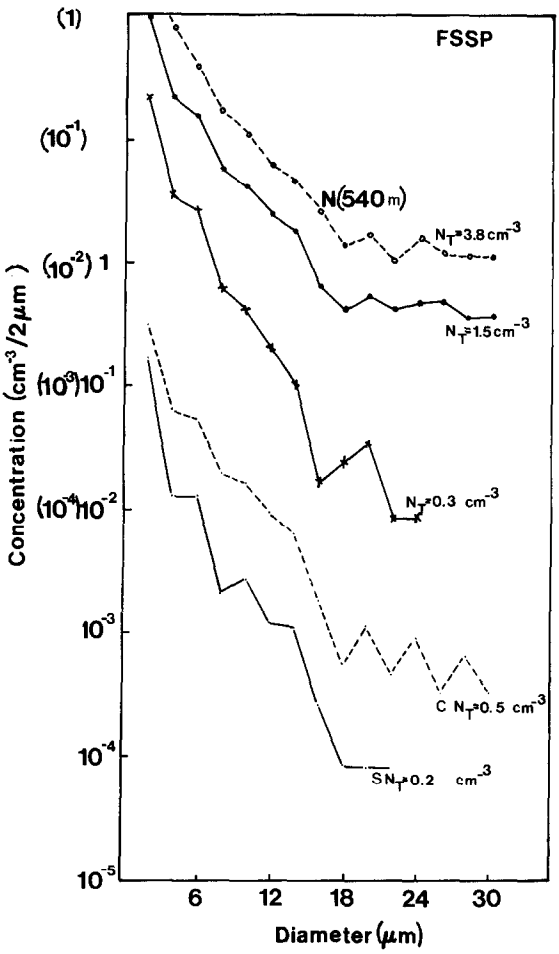

Fig. 13. Size distribution of aerosols using FSSP for Electra (S), (C) and (N). Ordinate for Electra (N) is shown in parenthesis. Remaining legend same as Fig. 12.

as much as 3.8 cm^{-3}. The high value at 540 m was obtained apparently, because the flight occurred within a cloud in the vicinity of its base.

Readings from the other two probes, X-200 and Y-200, were shown only at 540 m where a cloud existed. Thus, a high count of 287 L^{-1}, was registered by X-200 (Fig. 14). Fig. 15 shows the raindrop size distribution. The total count was small possibly because the larger drops were not formed yet.

Fig. 16 shows the ASAS measurements at Electra East and West. This figure is similar to Fig. 12 in that an exponential fall of concentration was experienced as bigger (greater than 0.8 μm diameter) particles were measured. It shows weaker concentrations than Fig. 12 because the East and West runs were executed within clouds. Electra East showed nearly similar distributions at all three levels where deep cumulus clouds existed. The average N_t value (23 cm^{-3}) of all six flights of 24 June within clouds was smaller than that of five

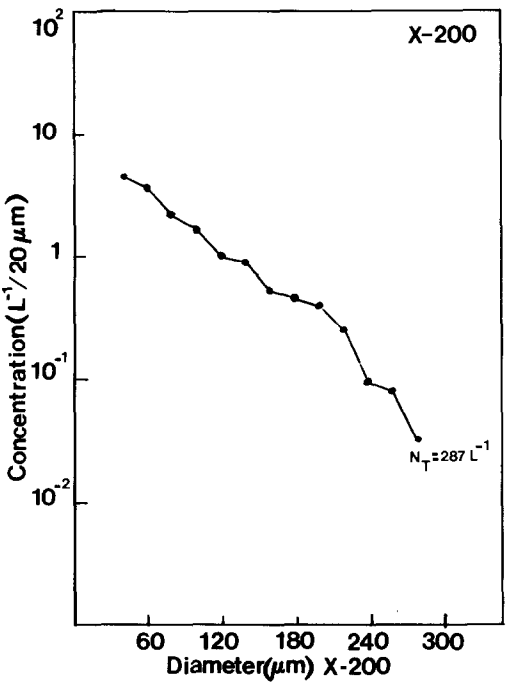

Fig. 14. Size distribution of cloud droplets for Electra (N) based on the X-200 probe at 540 m within the cloud but close to its base. Notice the high total concentration indicating that the cloud is still forming.

flights of 20 June (44 cm^{-3}) underneath clouds. This was apparently, because of the higher elevation of flights on 24 June. In general, a decrease of total concentration with height was shown in East and West flights.

The corresponding FSSP measurements were shown in Fig. 17. The Electra East had only small N_t values at 540 m, but nearly the same values in the middle and at the top of the clouds. The spectral distribution showed many small drops existing near the base, but developing into slightly larger amounts at higher elevations. The 16 mm camera pictures helped us to estimate the cloud tops around 1600 m.

At Electra West the FSSP concentration (Fig. 17) was low at 590 m and 1610 m with higher values at 1000 m elevation. The spectra showed that at the 590 m and 1610 m elevations, small drops existed in plenty, but the middle level (1000 m) showed a rise in the overall population. Tables 4 and 5 show that relatively, strong updrafts existed in the middle level of the cloud population (East and West) supporting the growth of small drops. Table 5 also shows that the Electra West developed stronger updrafts than Electra East (Table 4). Based on the FSSP spectral distributions we conclude that, since Electra East developed at 1000 and 1610 m a lesser fall of concentration with size than the counterparts at West, the eastern cloud system had already attained maturity while the western one had yet to grow.

6. Vertical velocity measurements

Gust probe measurements of vertical velocity were obtained during the constant altitude runs. Using these, one could relate updraft and downdraft intensities with convective activity

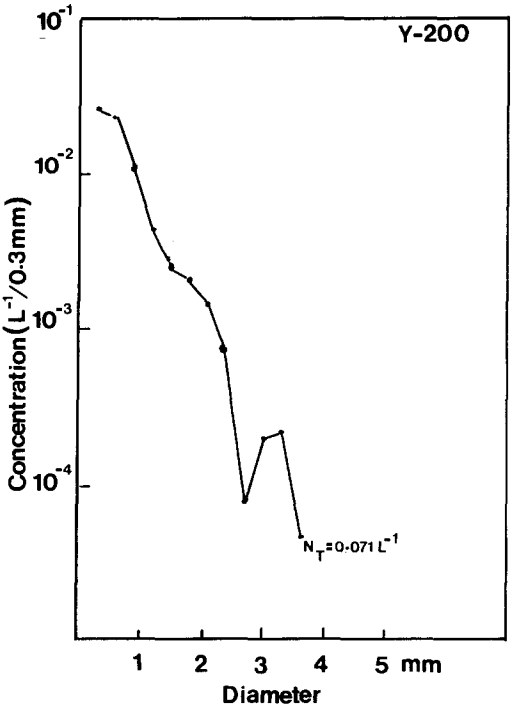

Fig. 15. Size distribution of raindrops for Electra (N) based on the Y-200 probe at 540 m within the cloud but close to its base. Precipitation (mm) sized particles are still forming accounting for the small total concentration.

and possibly with drop-size distributions. The identification technique of draft intensities follows LeMone and Zipser (1980) and Benson and Rao (1987). Basically, convective events were divided into two categories: drafts requiring that vertical velocity be continuously positive or negative for 500 m and should exceed an absolute value of 0.5 m s^{-1} for one second; and cores requiring that upward or downward vertical velocity be continuously greater than an absolute value of 1 m s^{-1} for 500 m. Mean updraft or downdraft vertical velocities (w) and cores were computed using

$$W=\frac{1}{N}\sum_{i} W_i$$

where N is the number of vertical velocity measurements in an updraft or downdraft and W_i is the individual vertical velocity observation. Processed W_i data were obtained at a rate of one sample per second.

Since exploration of convection was not the main objective of the aircraft maneuvers for these two days, it is possible that the updraft and downdraft intensities were underestimated. Nevertheless, some of these observations were presented because of the uniqueness of the data set. Only the structures belonging to Electra East and West were discussed because they covered cloud levels more adequately.

Table 4 shows the vertical velocity parameters for Electra East and Table 5 for Electra West on 24 June. The W represents the mean vertical velocity for the sample. The mean of

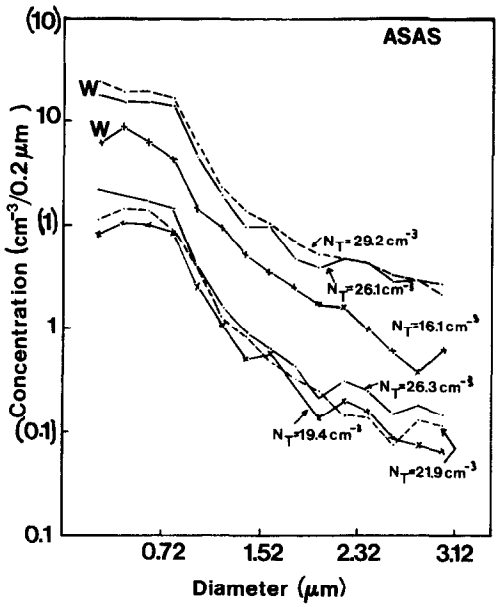

Fig. 16. Size distribution of aerosols using ASAS for Electra East and West for 24 June. Ordinate for Electra West is shown in parenthesis. Curves pertinent to West are labelled (*W*) and solid represents 540 m for East and 590 m for (*W*); dashed, 1000 m; and stars, 1610 m. All runs took place in clouds. Total number concentrations (*N* cm^{-3}) are also shown for each run. See Figs. 3 and 4 for the locations of Electra East and West.

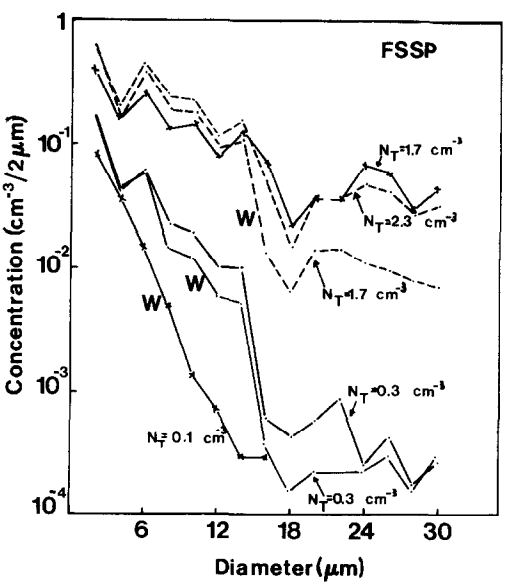

Fig. 17. Same as Fig. 13, except it relates to 24 June. Curves pertinent to West are labelled (*W*). Remaining legend same as Fig. 16.

Table 4
Some characteristic parameters of mean updrafts (U) and downdrafts (D) in the Electra East area on 24 June 1979

Height m	U or D	Sample size	Mean W (ms^{-1})	Mean of individual max W (ms^{-1})	Diameter (m)
540	U	8	0.36	0.71	1337
540	D	2	0.45	−0.80	550
1000	U	2	0.52	0.87	1250
1000	D	3	0.54	−1.19	1300
1610	U	3	0.33	0.72	3433
1610	D	3	0.30	−1.00	1033

Table 5
Some characteristic parameters of mean updrafts (U), downdrafts (D) and cores in the Electra West area on 24 June 1979

Height m	U or D	Sample size	Mean W (ms^{-1})	Mean of individual max W (ms^{-1})	Diameter (m)	Core sample size	Core W_{max} (ms^{-1})	Core diameter (m)
590	U	4	1.12	1.96	4650	7	1.52	1385
590	D	5	0.62	0.96	−3940	0	No	No
1000	U	2	1.37	1.71	6300	1	1.49	5400
1000	D	11	0.60	1.06	−2790	1	1.13	1000
1610	U	2	0.43	0.77	2160	0	No	No
1610	No Downdrafts							

individual maximum W_i, however, represents an average of the maximum found for each sample. The 590 m level for the West had developed four updrafts and five downdrafts with higher values than those found for the East at 540 m. In addition, this level developed seven cores of rising motion. The 1000 m level in the West registered two updrafts and one ascent core and 11 downdrafts and one descent core. At 1610 m two updrafts were detected. While a one-to-one correspondence between microphysics and vertical velocity is not easy to be found, the FSSP observations (Fig. 17) in both East and West show a relative maximum at the middle level where ascent (Tables 4 and 5) was also a maximum. This result appears consistent with the hypothesis of Sivaramakrishnan (1961) that a discontinuity in the updraft rate with maximum occurring at a certain level was responsible for a larger number of drops of a certain size compared with drops of sizes next, below, or above.

Although the West revealed a more convectively disturbed area than the East in terms of vertical velocities, the drop-size concentrations and their distributions did not show the higher values expected of it. Similarly, despite their better organizational appearance the eastern system did not register stronger vertical velocities. It is possible that the eastern system had already matured.

7. Conclusions

The measurements discussed above represent a unique set of in situ observations over the Arabian Sea when convection was present. In the following are these conclusions:

(1) The ASAS values were typically 30 cm^{-3} in the boundary layer, while the FSSP were much smaller (0.01 cm^{-3}). However, faster increases in FSSP values were seen overtaking the ASAS at about 1500 m. In general, saturation conditions call for an increased count of FSSP.
(2) The airmass in which measurements were taken appeared to be homogeneous as discussed by the uniformity of the ASAS and FSSP readings.
(3) The aerosol concentrations as measured by the ASAS probe during the disturbed conditions were higher than similar measurements in suppressed conditions. Strong winds and significant convergence fields resulting in higher vertical velocities were responsible for such higher concentrations. These concentrations show exponential decreases with size.
(4) The FSSP probe registered about ten times higher concentration values within a cloud (close to its base) than in subcloud layers. A spectral exponential decrease with size was seen in the data.
(5) The X-200 probe registered a higher count within a cloud near its base than that measured by the Y-200 probe showing that the cloud was still in the formative stage. This deduction was consistent with flight log wherein the observers found numerous build ups.
(6) Young cumulus clouds in the Central Arabian Sea in Electra West area measured higher FSSP concentrations in the middle level (1000 m) than either at the base or near the top. Such a distribution appears consistent with the vertical profile of updrafts as measured by the research aircraft which showed maximum values occurring at a certain level within the cloud. Obviously, such a level acts as a barrier (Sivaramakrishnan, 1961) to falling raindrops of a certain size and would cause a maximum concentration of drops belonging to a particular size group. Entrainment and mixing with the environmental air would make the drop concentrations diluted near the base, top, and lateral walls of the cloud.

In view of the possible association between El Niño and the world-wide weather, in particular, the Indian monsoon rainfall, more studies of the microphysical characteristics of clouds should be made over the monsoonal seas.

Acknowledgements

Both authors wish to thank Ms. Pamela Stephens of the National Science Foundation and Keith Griffith of NCAR for making the Summer MONEX PMS data available to them and Dr. T.H. Hor for computing the vertical velocity parameters from the original MONEX data tapes. Ridwan Tamin wishes to thank the Agency for the Assessment and Application of Technology (BPP Teknologi), Government of Indonesia for a scholarship to pursue graduate studies at Saint Louis University. Jeanne Mueller typed this article. Dr. Daniel Breed of NCAR provided comments on an initial version of this article.

References

Baumgardner, D., 1987. Corrections for the response times of particle measuring Probes. Sixth Symp. Meteorological Observations and Instrumentation, Jan 12–16, 1987, New Orleans, LA. Am. Meteorol. Soc., Boston, MA, pp. 148–151.

Baumgardner, D., 1989. Airborne Measurements for Cloud Microphysics. Research Aviation Facility Bull., 24. Natl. Center Atmos. Res., Boulder, CO 80307, 22 pp.

Benson, L.J. and Rao, G.V., 1987. Convective bands as structural components of an Arabian Sea convective cloud cluster. Mon. Weather Rev., 115: 3013–3023.

Cerni, T.A., 1983. Determination of the size and concentration of cloud drops with An FSSP. J. Clim. Appl. Meteorol., 22: 1346–1355.

Ellingson, R.G. and Serafino, G.N., 1984. Observations and calculations of aerosol heating over the Arabian Sea during MONEX. J. Atmos. Sci., 41: 575–589.

Fein, J. and Kuettner, J., 1980. Report on the Summer MONEX field phase. Bull. Am. Meteorol. Soc., 61: 461–474.

Hastenrath, S., 1991. Climate Dynamics of the Tropics. Kluwer, Dordrecht, 488 pp.

Holt, T. and Raman, S., 1985. Variation of turbulence in the marine boundary layer over the Arabian Sea during Indian southwest monsoon (MONEX 79). Boundary-Layer Meteorol., 37: 71–87.

Knollenberg, R.G., 1981. Techniques for probing cloud microstructure. In: P.V. Hobbs and A. Deepak (Editors), Clouds, their Formation, Optical Properties, and Effects. Academic Press, NY, pp. 15–91.

LeMone, M.A. and Zipser, E.J., 1980. Cumulonimbus vertical velocity events in GATE. Part I: Diameter, intensity and mass flux. J. Atmos. Sci., 37: 2444–2457.

Meyer, W.D. and Rao, G.V., 1985. Structures of the monsoon low-level flow and the monsoon boundary layer over the east Central Arabian Sea. J. Atmos. Sci., 42: 1943.

Podzimek, J., 1973. Contribution to the question of condensation nuclei formation on the seashore. J. Atmos. Res., 4: 137–152.

Pruppacher, H.R. and Klett, J.D., 1987. Microphysics of Clouds and Precipitation. Reidel, Dordrecht, 714 pp.

Rao, G.V. and Hor, T.H., 1991. Observed momentum transport in monsoon convective cloud band. Mon. Weather Rev., 119: 1075–1087.

Sivaramakrishnan, M.V., 1961. Studies of raindrop size characteristics in different types of tropical rain using a simple raindrop recorder. Indian J. Meteorol. Geophys., 12: 189–216.

Spyers-Durran, P., 1993. Private communication. NCAR Research Aviation Facility.